TECHNICAL INVESTIGATION OF A PYROPHORIC EVENT INVOLVING
CORROSION PRODUCTS FROM HEU ZPPR FUEL PLATES

Terry C. Totemeier
Argonne National Laboratory
Idaho Falls, ID 83403-2528
(208) 533-7458

ABSTRACT

A pyrophoric event recently occurred which involved corrosion products collected from highly-enriched uranium (HEU) fuel plates used in the Zero Power Physics Reactor (ZPPR). This paper summarizes the event and its background, and presents the results of an investigation into its source and mechanism. The investigation focused on characterization of corrosion product samples similar to those involved in the event using thermo-gravimetric analysis (TGA). Burning curve TGA tests were performed to measure the ignition temperature and hydride fractions of corrosion products in several different conditions to assess the effects of passivation treatment and long-term storage on chemical reactivity. The hydride fraction and ignition temperature of the corrosion products were found to be strongly dependent on the corrosion extent of the source metal. The results indicate that the energy source for the event was a considerable quantity of uranium hydride present in the corrosion products, but the specific ignition mechanism could not be identified.

1. INTRODUCTION

The oxidation behavior of uranium hydride (UH_3) formed as a product of the corrosion of U metal by water vapor is currently of interest due to the extended underwater storage of certain metallic spent nuclear fuels (SNF) and the anticipated long-term dry storage of SNF and U metal. The results of general characterization and oxidation testing of U metal corrosion products bearing significant fractions of UH_3 have recently been reported.[1-3] The products were collected from highly enriched uranium (HEU) metal fuel plates used in the Zero Power Physics Reactor (ZPPR) that corroded during extended vault storage.

A pyrophoric event involving similar corrosion products recently occurred at Argonne National Laboratory – West (ANL-W). The corrosion products had been passivated at room temperature and stored in air for a period of months.

This paper summarizes the event and its background, and presents the results of an investigation of its source and mechanism. The investigation primarily focused on characterization of corrosion product samples similar to those involved in the event using thermo-gravimetric analysis (TGA). Burning curve TGA tests were performed to measure the ignition temperature and hydride fractions of corrosion products in several different conditions to assess the effects of passivation treatment and long-term storage on chemical reactivity. Characterization was performed on corrosion products in three different conditions: immediately after separation from the source metal, after low-temperature passivation, and after low-temperature passivation and vault storage. The corrosion products were also characterized using X-ray diffraction (XRD) and BET gas sorption techniques.

2. BACKGROUND – PYROPHORIC EVENT

As stated above, the pyrophoric event involved corrosion products collected from HEU metal fuel plates used in ZPPR. The corrosion products, while nominally uranium oxide (UO_{2+x}), are known to bear a significant fraction of uranium hydride (UH_3). The corrosion products formed during extended vault storage of the fuel plates over a 12-year period. The history of the ZPPR fuel plate corrosion problem and an initial characterization of the corrosion products is detailed in Refs. 1 and 2. The unique storage configuration was the root cause of the severe corrosion—the U metal plates were tightly clad in stainless steel jackets with porous metal endplugs. The porous nature of the endplugs allowed access of ambient gas to the U, and the presence of the cladding created a crevice environment which supported the formation of UH_3 as a product of the reaction of water vapor with U metal.

The corroded plates were identified as a storage vulnerability by the U.S. Department of Energy (DOE) in a 1993 assessment.[4] In order to address the vulnerability and recycle the HEU present in the plates, a processing scheme for separation of useful uranium metal from the cladding and

DISCLAIMER

DISCLAIMER

Portions of this document may be illegible in electronic Image products. Images are produced from the best available original document

the corrosion products was developed and implemented. The procedure entailed decladding the plates in an inert atmosphere glovebox and separating the loose corrosion products from the metal coupons. After separation, the metal coupons were collected and induction cast into a single large ingot. The uranium metal was eventually used as feedstock for research reactor fuel.

The separated corrosion products underwent a passivation procedure intended to prevent pyrophoric events during subsequent handling and vault storage. In a pass-through Ar glovebox containing approximately 3% O_2, the products were ground into a fine powder using a mortar and pestle, spread into a thin layer, and exposed to the O_2-bearing environment for a minimum of two hours. The products were then transferred out of the glovebox to an enclosed air hood. Inside the hood the passive nature of the products was verified by vigorous agitation (stirring and pounding with a screwdriver) prior to their placement into a container (food-pack can) for vault storage. The corrosion products were stored with the intention that they would eventually be fully converted to oxide using a higher-temperature process. This procedure was used to process 376 kg of HEU over the course of about 1 year; 4.2 kg of corrosion products were separated, passivated, and placed into vault storage.

Because a separate, quart-size food-pack can was used for each casting batch (usually corresponding to 40 plates), the corrosion products collected during processing were distributed in 35 cans, each bearing less than 250 g. It was desired to consolidate the corrosion products into fewer containers to conserve storage space in the vault. Six food-pack cans were transferred at a time into an enclosed air hood. The contents of 13 food-pack cans were emptied into a large steel consolidation can in this manner without incident. At this point the consolidation can was approximately 75% full. As the contents of the 14th can were being poured into the consolidation can, the material from this can began sparking. Flames quickly formed above the material in the consolidation can and in the 14th food-pack can.

Attempts to extinguish the fire using a commercial retardant containing sodium chloride and magnesium aluminum silicate (Met-L-X®, Ansul Fire Protection) were unsuccessful because a gas stream eminating from the burning powder in the consolidation can ejected the retardant. The fire eventually self-extinguished without damage to the hood or spread of contamination outside the hood. Later inspection of the area revealed that corrosion product material had been expelled from the consolidation container, which had discolored due to the heat of the burning powder.

An investigative team identified the direct cause of the event as a failure to passivate the corrosion products in at least one of the food-pack cans. However, the team could not conclusively identify the mechanism by which burning was initiated. Two possible scenarios were presented. The first was a thermal excursion scenario whereby the tall geometry of the consolidation can led to ignition by preventing adequate heat removal from slowly oxidizing powder in the can. In the second scenario, the 14th food-pack can was assumed to be the ignition source, implying that the material in this can was different than that in the previous 13 cans. Additional experiments were recommended to better understand the ignition mechanism, the nature of the corrosion products, and the vulnerability of the 21 cans of corrosion product remaining in the vault.

3. EXPERIMENTAL PROCEDURES

A. Materials Analyzed

The objective of this investigation was to measure the properties of the ZPPR corrosion products for different conditions. Measuring the properties of the corrosion products at each stage of the passivation and storage process increases the understanding of how the material evolved, and enables a better analysis of the fundamental causes of the pyrophoric event to be made. The variation in properties with corrosion extent of the source plates was also determined for each condition. For all of the different conditions described below, the extent of corrosion was quantified as the mass of loose corrosion product divided by the total uranium mass of the plate or plates from which the corrosion products were collected.

1. Unpassivated Products. The first condition for which the properties of the corrosion products were measured was immediately after de-cladding of the plates and separation of the corrosion products from the metal coupons. A study of the corrosion products in this condition has been previously reported.[3] Additional unpassivated corrosion products were sampled and analyzed to better determine the effect of room temperature passivation on the corrosion product characteristics. Ten plates which showed moderate corrosion were selected and divided into two sets of five. The plates were de-clad in a glovebox with a pass-through Ar atmosphere, and the corrosion products collected from each set were combined into two separate "batches." The average corrosion extents of the source plates for the two batches were 1.16% and 1.41%. A two-gram sample of the corrosion products in the unpassivated condition was taken from each batch immediately after decladding of the plates.

2. Passivated Products. After initial sampling, the two batches of corrosion products were passivated. The O_2 content in the glovebox was increased to 3.5 vol.% by admitting a small flow of air. The two batches were separately ground to a uniform powder using a mortar and pestle and then left to sit in the O_2-containing environment for two hours. A second set of samples for TGA analysis was then taken from the passivated corrosion products.

3. Vault-Stored Products. Only 14 cans of corrosion products generated during the ZPPR fuel processing campaign were involved in the pyrophoric event, and 21 cans of nearly identical material remained in the vault. This material was collected from source plates with a broad range of corrosion extents, and hence the effect of corrosion extent could be readily quantified for this condition. TGA tests to measure the ignition temperature and hydride fraction of the vault-stored products were performed on samples from every can; XRD and BET analyses were performed on samples from selected cans.

B. Analysis Procedures

BET gas sorption analysis was performed on five samples of corrosion products in the vault-stored condition to compare their specific surface areas with those obtained for unpassivated powders in the earlier study.[3] The corrosion extents for the five samples ranged from 0.3 to 1.8. Analysis was performed using a Quantachrome Quantasorb® analyzer and standard BET techniques with Kr gas as the adsorbate, He gas as the carrier, and N_2 gas for calibration. Adsorption was carried out at liquid N_2 temperature; three consecutive measurements were made on each sample.

A modified Shimadzu TGA-51H analyzer located in a purified Ar glovebox was used to measure the oxidation kinetics and hydride content of the corrosion product powders. The standard test performed was the burning curve test, in which a 200 mg sample is heated at 15°C/min in a flowing Ar-20%O_2 atmosphere while the sample weight and furnace control thermocouple temperature are monitored. Ignition of the sample is clearly indicated by a sharp, simultaneous increase in both values; the ignition temperature is defined as the furnace temperature at this point. The sample is oxidized to completion, indicated by a stable sample weight. For samples which are known to contain UH_3, the total weight change during burning is used to calculate the fraction of UH_3 in the sample via the stoichiometry of the UH_3-O_2 reaction.

Isothermal oxidation tests were also performed. In an isothermal test, the sample is heated to the test temperature in a pure Ar atmosphere. When the test temperature is reached and stabilized, an Ar-30%O_2 reacting gas is admitted into the sample chamber. Mixing of the reacting gas with a pure Ar purge gas reduces the O_2 concentration in the sample chamber to 20%. The weight of the sample is recorded for the duration of the test. Isothermal oxidation tests performed in this investigation were typically 300 or 600 minutes long.

XRD was used for identification of metal, oxide, and hydride phases present in the corrosion product samples. The XRD test matrix and results are shown in Table 1. For samples that contained hydride, standardless analysis was performed using Sietronics phase analysis software to quantify the fractions of hydride and oxide for comparison with the results of the TGA tests. Diffraction was performed on a Scintag X1 powder diffractometer using Cu K-alpha radiation.

3. RESULTS

A. Specific Surface Areas

The specific surface areas of the five vault-stored corrosion product samples were essentially identical to those of the unpassivated products. The specific surface areas for all samples fell within the range of 0.5 to 1.0 m²/g, with the majority of the values approximately 0.7 to 0.8 m²/g. There was no effect of corrosion extent on specific surface area.

B. Burning Curve Reactivity

Figures 1 and 2 are plots of hydride fraction and ignition temperature as a function of corrosion extent for all conditions. There is considerable scatter, but ignition consistently occurred for corrosion extents above 1.2% and consistently did not occur for corrosion extents below 0.7%. For samples which ignited, the hydride fraction is roughly linearly dependent on corrosion extent. Ignition temperature is less strongly dependent on corrosion extent. Ignition temperature decreases with increasing corrosion extent to 1.2%, but is relatively independent of corrosion extent above 1.2%.

As shown in Figs. 1 and 2, there is little difference in hydride fraction or ignition temperature between the three different corrosion product conditions. For both parameters, the data for the three conditions fall within the same scatterband. Additionally, there was no change in ignition temperature or hydride fraction for the samples taken immediately before and after the passivation procedure.

Table 1. XRD Results Summary

Material ID	Corrosion Extent (%)	Phases Identified	Wt.% UH₃ (XRD)	Wt.% UH₃ (TGA)
Unpassivated Product				
Plate 2249	0.64	UO_{2+x}*, UH_3	3	No Ignition
Plate 2652	1.98	UO_{2+x}, UH_3	47	29-39
Vault-Stored Product				
SB97-1	0.33	UO_{2+x}, UH_3	4	No Ignition
RAM97-21/22	0.76	UO_{2+x}, UH_3	9	4-5
BWHEU-F-IC008	0.85	UO_{2+x}, UH_3	4	No Ignition
RAM97-1/2	0.92	UO_{2+x}, UH_3	4	No Ignition
RAM97-9/10	1.07	UO_{2+x}, UH_3	18	14-17
RAM97-23/24	1.80	UO_{2+x}, UH_3	26	22-25
BWHEU-F-IC009	1.83	UO_{2+x}, UH_3	42	27-29
Vault-Stored Product After Burning Curve Testing				
BWHEU-F-IC008 Oxidized to 620°C	0.85	U_3O_8	N/A	N/A
BWHEU-F-IC009 Oxidized to 250°C	1.83	UO_{2+x}, major U_3O_8, minor	N/A	N/A

*: UO_{2+x} denotes oxide which may be UO_2, U_3O_7, or a mixture of both.

Table 2. Results of Burning Curve Tests on Pre-oxidized Vault-stored ZPPR Corrosion Products

Test	Material ID	Pre-Oxidation Conditions			$T_{ignition}$ (°C)	$\Delta T_{ignition}$[a] (°C)
		Temp. (°C)	Time (min)	% UH₃ Reacted		
FMFVLT76	BWHEU-F-IC009	50	600	1.5	151	−12
FMFVLT78	BWHEU-F-IC009	75	600	3.1	173	+10
FMFVLT72	BWHEU-F-IC009	100	600	14	180	+17
FMFVLT63	BWHEU-F-IC009	125	240	23	181	+18
FMFVLT65	BWHEU-F-IC009	125	240	24	159	−4
FMFVLT67	BWHEU-F-IC009	125	480	38	188	+25
FMFVLT74	BWHEU-F-IC009	150	240	66	208	+45
FMFVLT84	RAM97-9/10	50	600	0[b]	169	+6
FMFVLT80	RAM97-9/10	100	600	8.0	183	+20
FMFVLT82	RAM97-9/10	125	600	19	187	+24
FMFVLT86	RAM97-9/10	150	300	62	214	+51

a: Difference from average baseline ignition temperature for corresponding material.
b: No measurable weight gain.

C. Isothermal Oxidation Kinetics

Figure 3 is an Arrhenius plot of oxidation rates versus reciprocal temperature for isothermal tests on unpassivated and vault-stored corrosion products. Tests were performed on corrosion products from two cans with different corrosion extents. The oxidation rates shown are best linear fits to weight gain versus time data for each test normalized by reacting surface area, as described in Ref. 3. The shapes of the weight gain versus time curves for tests on the vault-stored products were similar to those for tests on unpassivated products—the rate of weight gain slowly decreased throughout each test. The UH₃ surface area used to normalize the weight gain data was computed as the product of the BET specific area, the sample mass, and the hydride fraction.
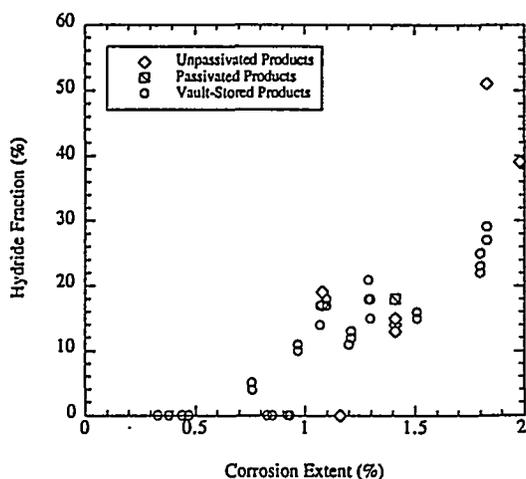
Fig. 1: Plot of hydride fraction versus corrosion extent for ZPPR corrosion products. Data points with a hydride fraction of zero did not ignite.
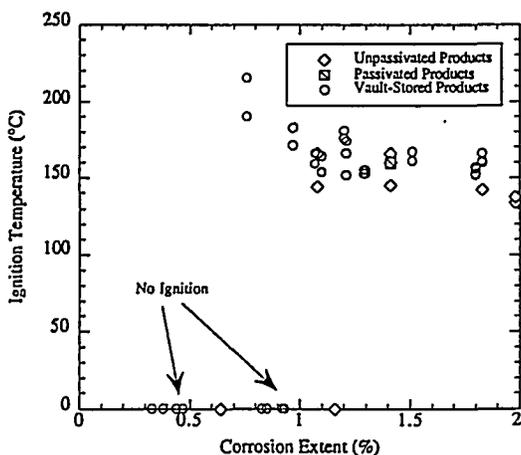

Fig. 2: Plot of ignition temperature versus corrosion extent for ZPPR corrosion products. Data points with an ignition temprature of zero did not ignite.

There was no significant difference in the oxidation rates measured for the two material conditions. The data for the two cans of vault-stored corrosion products lie within the scatterband for the unpassivated products.

The effect of pre-oxidation on subsequent burning curve reactivity was assessed by performing burning curve tests on the partially oxidized samples from the isothermal tests. The results of these tests are presented in Table 2. Significant pre-oxidation resulted in an increase in ignition
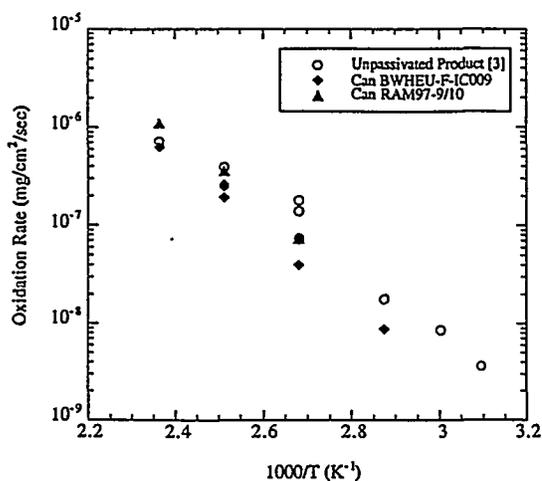

Fig. 3 Plot of isothermal oxidation rates versus reciprocal temperature for ZPPR corrosion products.

temperature. For material from can BWHEU-F-IC009, the ignition temperature increased from 160°C to 208°C as a result of oxidation at 150°C. A similar increase was observed for material from can RAM97-9/10. The magnitude of the ignition temperature increase depended on the extent of pre-oxidation. Little increase was observed when the weight gain incurred in the isothermal test was low.

D. X-ray Diffraction

Table 1 summarizes the results of the XRD analyses. The phases identified in each sample are listed. For samples which contained oxide and hydride, the result of the quantitative analysis of the XRD pattern is shown, with the corresponding TGA result for comparison. For samples containing phases other than oxide and hydride, the major and minor peaks of the pattern are identified. Hydride peaks were observed for all unpassivated and vault-stored samples, even for those which did not ignite in TGA testing. The quantitative analysis results showed a dependence of UH_3 content on corrosion extent similar to that observed in TGA tests. The samples which did not ignite in TGA testing showed low hydride fractions in the XRD analysis.

4. DISCUSSION

A. Effect of Corrosion Extent on Properties

There was no effect of corrosion extent on the specific surface areas measured for unpassivated and vault-stored corrosion products. The specific surface areas were generally

between 0.7 and 1.0 m^2/g, regardless· of corrosion extent. Only one outlier from this range is present, at 0.5 m^2/g for a corrosion extent of 0.64%. The lack of an effect of corrosion extent on specific area was discussed in Ref. 3.

The ignition temperature and hydride fraction of the corrosion products were found to be strongly dependent on source metal corrosion extent. These effects are shown in Figs. 1 and 2. The dependence of hydride fraction on extent is a result of variations in the amount of localized corrosion for different plates. As documented in Ref. 1, the hydride component of the corrosion products (a black powder) tends to be associated with areas of severe localized corrosion, while light gray oxide flakes are associated with general corrosion. Plates with more localized corrosion (more hydride) tend to have a greater corrosion extent. Plates which do not have any areas of localized corrosion (and hence little hydride) typically have only a small amount of corrosion product (low corrosion extent).

The effect of corrosion extent on ·ignition temperature is related to its effect on hydride fraction. Ignition is defined by a balance between heat generation and loss; the strong dependence of oxidation rates on temperature results in rapid self-heating when the rate of heat generation due to oxidation exceeds the rate of·heat loss. Samples with higher hydride fractions have a greater heat generating capacity relative to the total mass of the sample, and so are expected to ignite at lower temperatures than samples with low fractions. Samples with very low hydride fractions may not ignite at any temperature, since the small amount of heat generated by oxidation of the hydride can be absorbed by a large quantity of intimately surrounding oxide.

The variation of ignition temperature with hydride fraction for samples which ignited is shown in Fig. 4. Ignition was not observed for hydride fractions less than 4%. Above 4% hydride, the ignition temperature decreases relatively quickly with increasing hydride fraction until 15% is reached, then decreases much more slowly (if at all) for hydride fractions greater than 15%. A possible explanation for the relative independence above 15% is that sufficient hydride is present that the ignition temperature is determined more by the intrinsic oxidation kinetics of the hydride than the inert nature of the oxide.

No effect of corrosion extent was observed for isothermal oxidation data below the ignition temperature. The data from corrosion products with four different corrosion extents (two plates and two vault-stored cans) fall into essentially the same scatterband on Fig. 3. Because the data presented in Fig. 3 has been normalized by hydride surface area, the effect of ' varying hydride fraction is accounted for. There is therefore no intrinsic variation in

low-temperature oxidation rate with corrosion extent. There is also no significant effect of storage condition.

The results of the XRD analyses of the corrosion products support the TGA findings. Reasonable agreement was found between hydride fractions computed using the weight gain in TGA tests and those computed using the XRD standardless quantitative analysis software. Some differences did exist—the values from XRD analysis were typically higher than from TGA analysis, and XRD detected the presence of hydride for all unpassivated and vault-stored corrosion products, even for those samples which did not ignite in TGA tests. The source of the discrepancy between the values obtained with the two techniques is currently unknown.
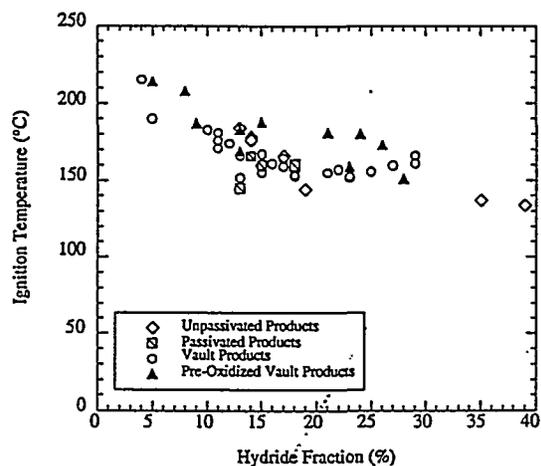

Fig. 4: Plot of ignition temperature as a function of hydride fraction for ZPPR corrosion products.

B. Changes in Properties Due to Passivation and Storage

Given the dependence of corrosion product properties on corrosion extent described above, any evaluation of changes in properties due to passivation and storage must account for corrosion extent. This is accomplished by comparing data from different conditions on plots of properties versus corrosion extent, where a significant difference is manifest as an outlying data point or curve. The data shown in Figs. 1 and 2 demonstrate the similarity of properties for unpassivated, passivated, and vault-stored corrosion products. All conditions fall into the same broad scatterband. The lack of an effect of the room-temperature passivation process on the ignition temperature or hydride fraction is confirmed by the results obtained from the two batches of corrosion product tested before and immediately after passivation, in which no change in UH$_3$ fraction or ignition temperature was observed.

The results of the burning curve tests on pre-oxidized, vault-stored corrosion products demonstrate that partial reaction of hydride does raise the ignition temperature. However, a large fraction of the hydride must be reacted, and the change in ignition temperature is relatively small. In the extreme case (test FMFVLT 86), reaction of 62% of the hydride present in the sample increased the ignition temperature by only 51°C, from the baseline value of 163°C to 214°C (Table 2). Reaction of lower fractions (~20%) increased the ignition temperature less than approximately 20°C. The increase in ignition temperature resulting from significant pre-oxidation can be accounted for by the reduction in hydride fraction. Reaction of hydride in an isothermal oxidation test lowers the net hydride fraction for the subsequent burning curve test. As shown in Fig. 4, ignition temperature increases with decreasing hydride fraction, especially for fractions less than 15%.

The lack of an effect of the low-temperature passivation step and results obtained in pre-oxidation tests indicate that true passivation—a significant reduction in reactivity due to formation of a thin, passive layer of oxide on the surface of a hydride particle—does not occur for ZPPR corrosion products. Passivation may not appear to occur for the ZPPR corrosion products because the UH_3 present is likely already passivated due to its formation in an oxidation process (as opposed to reaction with pure H_2 gas) and the intimate presence of oxide and water vapor. The similarity of ZPPR corrosion product ignition temperatures to those reported for "passivated" UH_3 by Longhurst, 140°C,[5] supports this argument. The experience with ZPPR corrosion products, however, demonstrates that "passivated" UH_3 with ignition temperatures exceeding 100°C may still ignite at room temperature under certain handling conditions.

C. Sources and Mechanisms for the Pyrophoric Event

The main issues that this study addressed were the cause of the pyrophoric event and the specific mechanism of ignition. The energy source is clear—the corrosion products contained a substantial quantity of UH_3 which reacted with air in the event. The ignition temperatures of the corrosion products were essentially the same as immediately following removal from the source plates; the material was not at all passivated relative to its initial condition. The specific mechanism by which ignition of the corrosion products occurred still cannot be conclusively identified. However, the data obtained in this series of tests can be used to analyze the mechanisms proposed by the investigative team—the thermal excursion scenario and the can 14 scenario.

In the thermal excursion scenario, oxidation slowly increases the temperature of the consolidated product to the ignition point because the tall cylindrical can prevents

effective heat loss from the powder. Simple analysis shows this scenario to be extremely unlikely. From Fig. 3, the rate of oxidation for the corrosion products at 25°C is 6×10^{-10} mg/cm^2/sec. For conservative values of specific area (1.0 m^2/g) and hydride fraction (20%), adiabatic heating due to oxidation results in a temperature increase of 2×10^{-5} K/sec. At this rate of increase, 13 hours are required for the powder to heat one degree. Since the consolidation operation was performed in less than 4 hours, the corrosion product could not have self-heated to the ignition point (at least 130°C). The thermal excursion scenario is therefore not plausible.

The second proposed scenario was that in which the 14th can was different than the previous 13. Three possibilities were presented: (1) the material in the 14th can was fundamentally different; (2) the material in the 14th can was improperly passivated; and (3) the material in the 14th can had changed (become more reactive) during storage. The results of this study indicate that there was no effect of the passivation step. Therefore, the material in can 14 could not have been inadequately passivated relative to the other cans. The results also indicate that an increase in reactivity did not occur as a result of storage. The material in can 14 was different, however, in that it was collected from source plates with a corrosion extent (1.8%) higher than any of the previous 13 cans. Therefore, can 14 likely had an ignition temperature lower than the other 13 cans and a higher pyrophoric potential.

Operator observations of the event indicated that the fire indeed appeared to initiate in the can 14 material, but the ignition source remains unidentified. Two possible "sparks" are static discharge or mechanical agitation during pouring of the powder. Also, the question of why the material did not ignite during stirring and handling in air prior to vault storage remains unanswered. This experience highlights the unpredictable nature of uranium hydride.

5. CONCLUSIONS

Hydride-bearing uranium metal corrosion products from ZPPR fuel plates involved in the March 13, 1998 pyrophoric event at ANL-W were characterized using TGA, XRD, and BET techniques. The following conclusions were reached:

1. The hydride fraction of corrosion products increased with increasing corrosion extent of the source plates. The ignition temperature of the corrosion products decreased with increasing corrosion extent and hydride fraction.

2. There was little change in corrosion product properties after passivation or long-term vault storage. The passivation step did not alter either the ignition temperature or the hydride fraction of the corrosion products.

3. Partial oxidation of the corrosion products decreased reactivity by increasing the ignition temperature, but a large reaction extent was required to achieve only a small increase in ignition temperature. Therefore, complete oxidation of the hydride is required to guarantee safe handling and storage.

4. The energy source for the pyrophoric event was a considerable quantity of UH_3 present in the corrosion products. No specific ignition mechanism could be conclusively identified, but the available evidence disproves a scenario in which the powder in the consolidation can slowly self-heated to the ignition point. The experience highlights the unpredictable nature of UH_3.

ACKNOWLEDGMENTS

REFERENCES

1. T.C. Totemeier, R.G. Pahl, S.L. Hayes, and S.M. Frank, "Characterization of Corroded Metallic Uranium Fuel Plates," *J. Nucl. Mater.*, **256**, 87 (1998).

2. T.C. Totemeier, R.G. Pahl, S.L. Hayes, and S.M. Frank, *Metallic Uranium ZPPR Fuel: Corrosion Characteristics and Corrosion Product Oxidation Kinetics*, Argonne National Laboratory Report ANL-98/11 (1998).

3. T.C. Totemeier, R.G. Pahl, and S.M. Frank, "Oxidation Kinetics or Hydride-Bearing Uranium Metal Corrosion Products," *J. Nucl. Mater.*, **265**, 308 (1999).

4. *Spent Fuel Working Group Report on Inventory and Storage of the Department's Spent Nuclear Fuel and other Reactor Irradiated Nuclear Materials and their Environmental, Safety, and Health Vulnerabilities*, U.S. Department of Energy Report (1993).

5. G.R. Longhurst, *Pyrophoricity of Tritium-Storage Bed Materials*, EG&G Idaho Report EGG-FSP-8050 (1988).